

NASA Technical Paper 1373

LOAN COPY: RETURN TO
AFWL TECHNICAL LIBRARY
KIRTLAND AFB, N.M.



Comparison of Calculated and Altitude-Facility-Measured Thrust and Airflow of Two Prototype F100 Turbofan Engines

Frank J. Kurtenbach

DECEMBER 1978

NASA



NASA Technical Paper 1373

Comparison of Calculated and Altitude-Facility-Measured Thrust and Airflow of Two Prototype F100 Turbofan Engines

Frank J. Kurtenbach
*Dryden Flight Research Center
Edwards, California*



National Aeronautics
and Space Administration

**Scientific and Technical
Information Office**

1978

COMPARISON OF CALCULATED AND ALTITUDE-FACILITY-MEASURED THRUST AND AIRFLOW OF TWO PROTOTYPE F100 TURBOFAN ENGINES

Frank J. Kurtenbach
Dryden Flight Research Center

INTRODUCTION

The Dryden Flight Research Center is involved in a flight program with the F-15 airplane that has as one of its objectives the study of airframe/propulsion system integration. This study requires an accurate knowledge of engine airflow and gross thrust. Therefore, the two F-15 F100-PW-100 engines to be used in the flight program were calibrated for thrust and airflow in the NASA Lewis Research Center Propulsion Systems Laboratory 4 altitude facility.

Engine test conditions were chosen to match the conditions proposed for the flight programs. The testing of the first engine (serial number P680059; hereafter 059) covered only a minimum of Mach number/altitude conditions through the center of the engine operating envelope. The second engine (serial number P680063; hereafter 063), considered the primary flight test engine, was tested at all except one of the 059 Mach number/altitude conditions and, in addition, at more extreme portions of the operating envelope.

The facility-determined performance for these two prototype engines is described in references 1 and 2.

This report compares the facility performance data for the two engines to the engine manufacturer's performance calculation model (ref. 3) and provides corrections that can be applied to the model so that it represents the test engines accurately over the full flight envelope.

The effects of inlet flow distortion and Reynolds number were examined along with hysteresis and engine degradation. The calibrated model calculation accuracy was compared with the uncertainty estimated from instrumentation uncertainty.

SYMBOLS AND ABBREVIATIONS

A	area, m^2
C_D	nozzle discharge coefficient
C_V	nozzle velocity coefficient
D	distortion parameter, $\frac{p_{t2_{max}} - p_{t2_{min}}}{p_{t2_{av}}}$, percent
EEC	engine electronic control
F_g	gross thrust, kN
FIGV	fan inlet guide vane angle, deg
FTIT	fan turbine inlet temperature, K
M	Mach number
N	engine component rotation speed, rpm
NPR	nozzle pressure ratio, p_{t7}/p_0
PR	pressure ratio, p_t/p
$PRQPR$	nozzle performance parameter (p. 19)
p	static pressure, N/cm^2
p_t	total pressure, N/cm^2
RNI	Reynolds number index, $\frac{\delta}{\theta^{1.24}}$
T	temperature, K
UFC	unified fuel control
W	mass flow, kg/sec

W_{fp}	primary (gas generator) fuel flow , kg/hr
W_{ft}	total (primary plus afterburner) fuel flow , kg/hr
γ	ratio of specific heats
δ	$= p_{t_2} / p_{sl}$
θ	$= T_{t_2} / T_{sl}$
σ	standard deviation, percent

Subscripts:

av	average
$core$	engine core
e	nozzle exit plane (engine station 8)
fac	facility
j	jet (engine station 7)
max	maximum
min	minimum
mod	model
sb	subsonic
sl	sea level
sp	supersonic
t	total

Facility and engine stations (figs. 1 and 3):

PL	inlet plenum
0	simulated free stream
1	inlet duct measurement position
2	engine inlet

2.5	fan exit
4.5	fan-turbine inlet
6	fan-turbine exit
6.5	augmentor liner
6.7	augmentor liner
6.9	augmentor liner
7	nozzle throat
8	nozzle exit

ENGINE DESCRIPTION

The F100-PW-100 engine (fig. 1) is a low bypass, twin spool, augmented turbofan. The engine has 13 compression stages, composed of a three-stage fan (which is driven by a low pressure two-stage turbine) and a 10-stage compressor (which is driven by a high pressure two-stage turbine). The engines have a high compression ratio and achieve improved performance and distortion attenuation

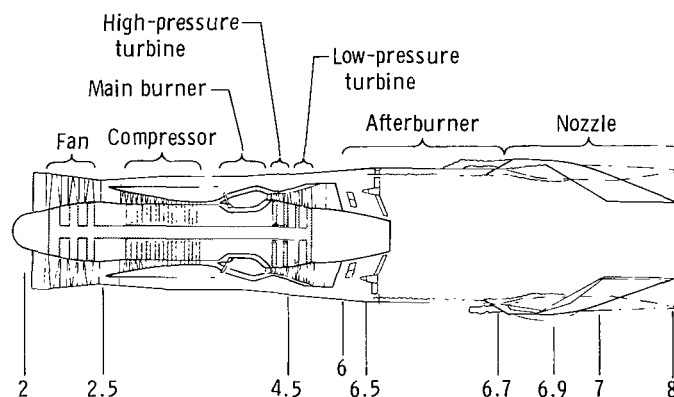


Figure 1. Schematic representation of prototype F100-PW-100 engine.

through the use of variable fan and compressor geometry. Continuously variable thrust augmentation is provided by a mixed-flow afterburner, which exhausts through a variable area convergent-divergent nozzle.

The engines tested are classified as prototype engines, series 2 7/8. The engines incorporate F100 series 2 cores (compressor, burner, and turbine), but include the series 3 improved stability fan with recessed splitter. In addition, they have control schedule differences from both the series 2 and 3 engines, and

they have series 2 actuated divergent nozzles, whereas the series 3 engines have free-floating nozzles.

The F100 engines are primarily controlled by a unified hydromechanical fuel and nozzle control (UFC), with supervisory control performed by an engine electronic control (EEC). One of the functions of the EEC is to limit minimum fan airflow to insure inlet stability. This is accomplished through the use of an airframe-supplied free-stream Mach number signal. Below Mach 0.90, the EEC allows engine operating power lever angle to go idle. The minimum allowable value increases linearly with Mach number to intermediate power at a Mach number of 1.4. It remains constant at this level for higher Mach numbers. The free-stream Mach number was electrically supplied to the EEC by the facility and could be changed manually. This provided the ability to operate below intermediate for supersonic test conditions.

The convergent-divergent nozzle has a divergent section scheduled as a function of nozzle throat area, A_j . One of two possible A_e versus A_j schedules is used to optimize thrust, depending on the free-stream Mach number: the low mode schedule is used for $M_0 < 1.1$, and the high mode schedule is used for $M_0 > 1.1$. For afterburning operation, the facility's ability to alter the Mach number allowed operation on either of the two nozzle area ratio schedules.

The ability to test at these nonstandard operating conditions provided additional test points which further verified the fluid mechanic and thermodynamic validity of the model.

TEST FACILITY AND EQUIPMENT

Altitude Test Facility

Figure 2 shows the F100 engine installed in the altitude facility. The facility provided a calibrated load cell thrust bed for determining actual gross thrust and a

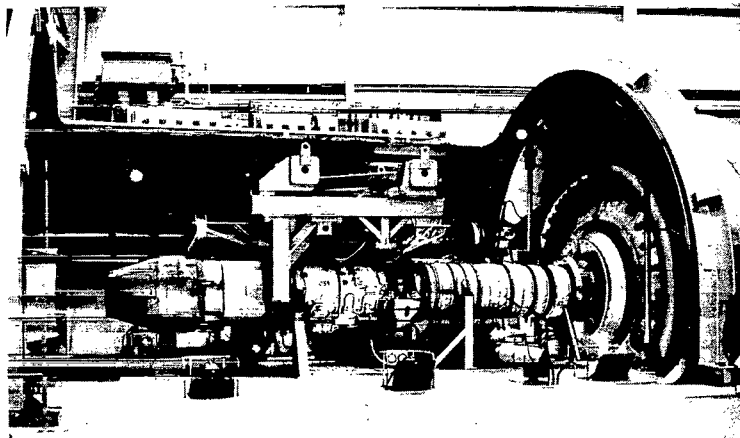


Figure 2. Prototype F100-PW-100 engine installed in facility.

specially instrumented inlet duct section for determining actual engine inlet mass flow. Further description of the facility can be found in references 1 and 2.

Distortion Screens

A different distortion screen was used for each engine, and the distortion test conditions for each engine were different. The distortion test for engine 059, which used screen 1, was conducted at a standard day temperature at Mach 0.80 at an altitude of 4020 meters. The distortion test for engine 063, which used screen 2, was conducted for a standard day temperature at Mach 0.89 and an altitude of 7380 meters. The distortion characteristics of the screens at the intermediate power airflow for these conditions are given in table 1. Further description of the screens can be found in references 1 and 2.

TABLE 1.—DISTORTION SCREEN CHARACTERISTICS AT TEST CONDITIONS

	Engine	
	059	063
Screen	1	2
Mach number	0.80	0.89
Altitude, m	4020	7380
$\frac{W\sqrt{\theta}}{\delta}$, kg/sec	99.12	101.82
D, percent	13.5	26.5

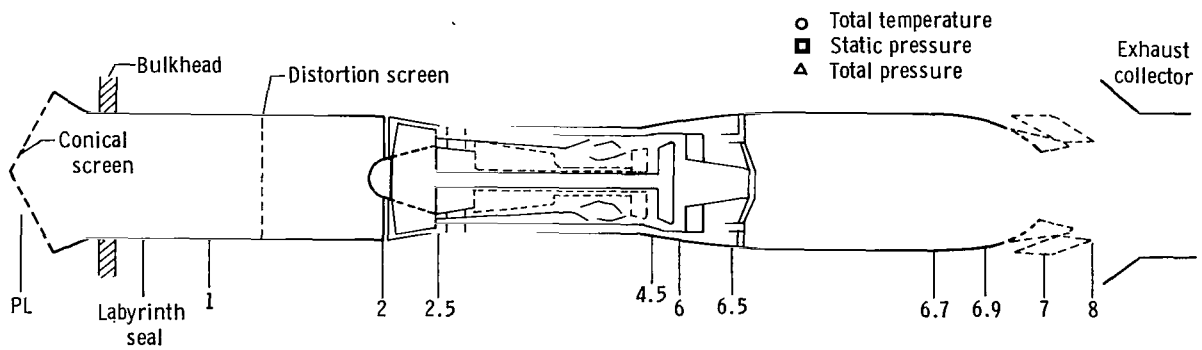
Instrumentation

The facility and engine station designations and the corresponding instrumentation are shown in figures 1 and 3. All instrumentation was capable of steady-state measurement only, and all engine rakes and probes were flight-qualified hardware. All pressures, with the exception of those at station 2.0 in the 059 tests, were measured with scanivalves that were mounted external to the test chamber.

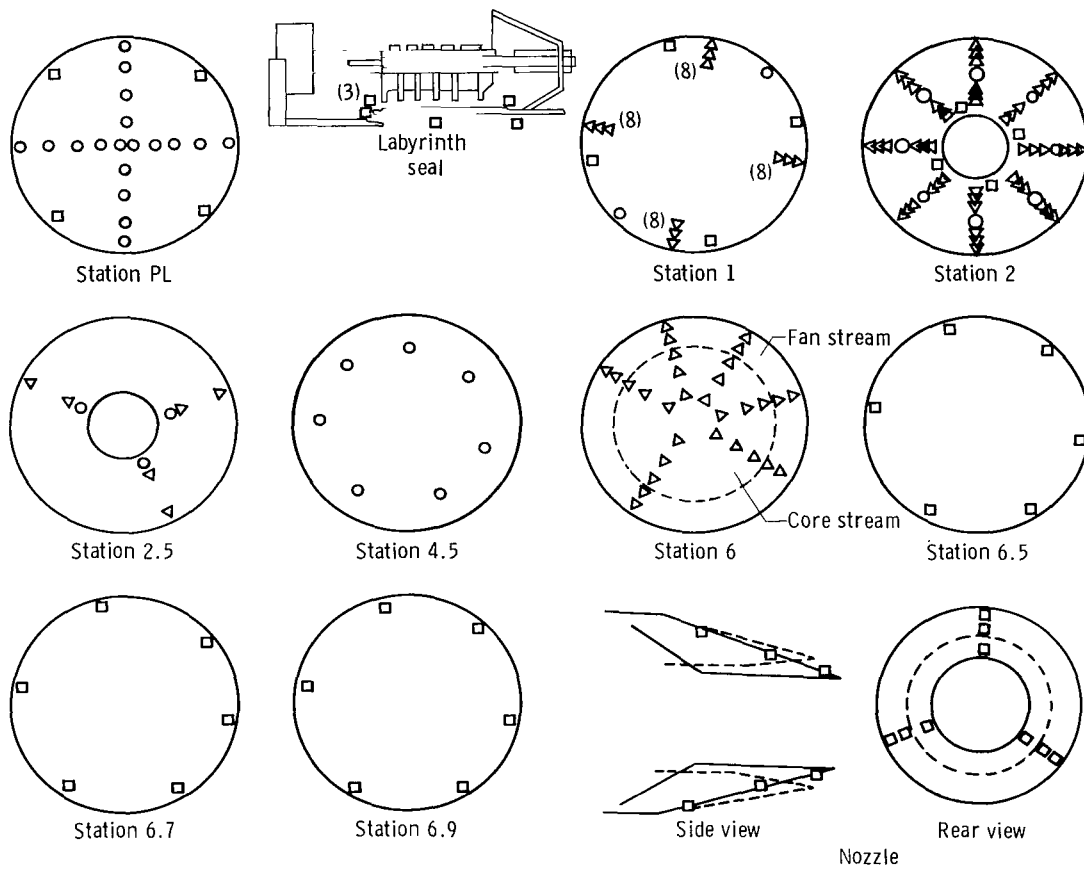
The average of the plenum total temperature measurements was used as engine inlet temperature.

Station 1 pressure instrumentation provided the facility value for engine face mass flow. Pressures were measured at the labyrinth seal to monitor for seal leakage.

The station 2.0 rake used for the 059 tests had transducers mounted in the hub. The hub was temperature controlled; however, shifts in temperature were still observed. A special test was performed to determine the change in average total pressure with hub temperature change, and the average pressure value was corrected accordingly. The correction was consistent with transducer average specification data, and the effect on the uncertainty of average total pressure was believed negligible. However, individual transducers could not be corrected for temperature, so the indicated distortion pattern for engine 059 was affected. Measurements made at stations 2.5, 6.5, 6.7, and 6.9 were not required for engine calibration.



(a) Station locations.



(b) Individual stations.

Figure 3. Engine instrumentation.

Station 4.5 instrumentation provided fan turbine inlet temperature. The instrumentation at station 6 consisted of an array of 30 total pressure probes mounted on six rakes.

Nozzle area was determined by the use of an engine-mounted linear potentiometer that was connected to the nozzle components downstream of the actuating cables. The potentiometer was air cooled to reduce calibration shifts due to temperature. Engine 063 had an additional potentiometer that was connected directly to the drive cable and was not air cooled. Only the air cooled linear potentiometer measurement was used in the gas generator gross thrust calculation.

Ambient exhaust pressure was determined from nine static pressure ports located on the exterior of the divergent section of the nozzle. All nine pressure values were in good agreement for all test conditions.

Table 2 lists pertinent performance measurements and the corresponding uncertainties. The uncertainty of p_{t_6} is $\pm 0.097 \text{ N/cm}^2$, which differs from the facility value of $\pm 0.026 \text{ N/cm}^2$. It was felt that this value better represented the measurement uncertainty due to probe design. A discussion of the altitude facility values for instrumentation uncertainty can be found in references 1 and 2.

TABLE 2.—PARAMETER UNCERTAINTY

	Uncertainty
N_1 , percent	± 0.1
p_0 , N/cm^2	± 0.026
p_{t_2} , N/cm^2	± 0.026
p_{t_6} , N/cm^2	± 0.097
T_{t_2} , K	± 1.78
A_j , percent	
Closed	± 3.30
Open	± 1.86
FIGV, deg	± 0.530
W_{fp} , kg/hr	± 22.7
W_{ft} , kg/hr	± 118.0

TEST CONDITIONS AND PROCEDURES

The test conditions are shown in table 3 and figure 4. After the selection of flight Mach numbers and altitudes, a representative inlet recovery value was chosen based on typical flight values. The recovery value was assumed to be constant for each facility Mach number/altitude condition, although in flight this value varies with engine mass flow.

TABLE 3.—TEST CONDITIONS

(a) Engine 059

Inlet flow	M_0	Altitude, m	p_{t_2} , N/cm ²	T_{t_2} , K	p_0 , N/cm ²	RNI
Uniform	0.80	4,020	9.27	296	6.14	0.89
Uniform	0.80	4,020	9.27	^a 284	6.14	0.93
Uniform	0.80	4,020	9.27	^a 313	6.14	0.83
Uniform	0.89	7,380	6.45	278	3.90	0.66
Uniform	1.20	12,100	4.54	279	1.90	0.46
Uniform	1.20	12,100	4.54	^a 290	1.90	0.45
Uniform	1.40	15,240	3.61	301	1.16	0.34
Distorted (screen 1)	0.80	4,020	9.27	296	6.14	0.89

^aNonstandard day.

(b) Engine 063

Inlet flow	M_0	Altitude, m	p_{t_2} , N/cm ²	T_{t_2} , K	p_0 , N/cm ²	RNI
Uniform	0.80	4,020	9.27	296	6.14	0.89
Uniform	0.89	7,380	6.45	278	3.90	0.66
Uniform	0.89	7,380	6.45	^a 295	3.90	0.62
Uniform	1.40	15,240	3.61	301	1.16	0.34
Uniform	0.90	13,720	2.48	252	1.48	0.29
Uniform	1.60	9,140	12.00	339	3.01	0.96
Uniform	2.00	15,240	8.56	390	1.16	0.58
Distorted (screen 2)	0.89	7,380	6.45	278	3.90	0.66

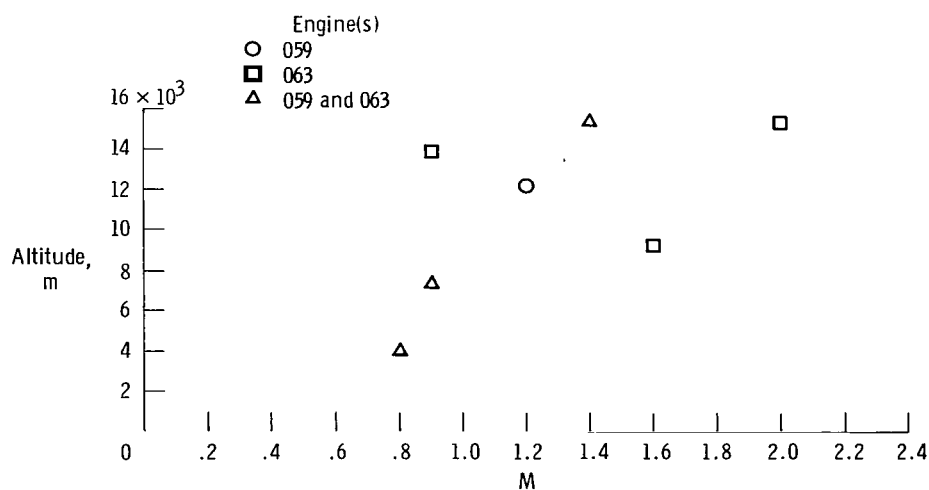
^aNonstandard day.

Figure 4. Test conditions.

The distortion tests were conducted at the same engine face average pressure and temperature as the uniform inlet tests to prevent a Reynolds number effect in the distortion data. This was achieved by increasing the facility plenum pressure to absorb the pressure loss across the screen.

The general test procedure was to establish a given Mach number/altitude condition in the facility with the engine at an appropriate operating condition. Data were acquired after every change of power lever angle as soon as the engine and facility were stable (after 1 minute minimum). Multiple data points were acquired for most engine operating conditions. In addition, some data were gathered with both sequentially increasing and sequentially decreasing steps of power lever angle to assess the presence of hysteresis in either the engine or the facility.

Data were gathered at power settings from idle to maximum afterburning for all Mach number/altitude conditions, with the exception of the Mach 0.80, 4020-meter and Mach 0.89, 7380-meter (standard day) conditions on engine 063. These two conditions were not tested with afterburner. Engine operation at power settings below intermediate was achieved for Mach numbers greater than 0.90 by manually adjusting the facility-supplied free-stream Mach number signal to the EEC to a value of 0.80. Besides eliminating the EEC-scheduled airflow bottoming and topping limits, this procedure also kept the nozzle area ratio schedule in the low mode. For most afterburning tests at Mach numbers of 1.20 or greater, data were acquired for both area ratio schedules by changing the Mach number signal to the EEC, providing additional data on nozzle coefficients.

Only a select number of points were used to show engine performance in references 1 and 2. In this report, all points at or following the first stabilized intermediate power point are used. This provided data of the type expected for the flight program, where engine stabilization times are minimal and hysteresis can be present.

The uniform flow tests provided 445 data points for engine 059 and 339 points for engine 063. This allowed an extensive repeatability analysis.

For engine 059, the Mach 0.80, 4020-meter, standard day, uniform inlet condition was the first test performed and was repeated as the last test, providing information on engine degradation over the 20 hours of engine operation.

ENGINE PERFORMANCE MODEL

The manufacturer's engine model (ref. 3 and fig. 5) is a gas generator analysis model which relies primarily on total pressure measurement and nozzle area for the determination of gross thrust. The model uses a combination of theoretical values, component test data, and full-scale engine data to generate the relationships necessary for the analysis.

First, corrected fan airflow is computed as a function of engine pressure ratio and corrected fan speed. The result is then corrected for inlet guide vane angle and Reynolds number. Station 6 total temperature, T_{t_6} , is computed as a

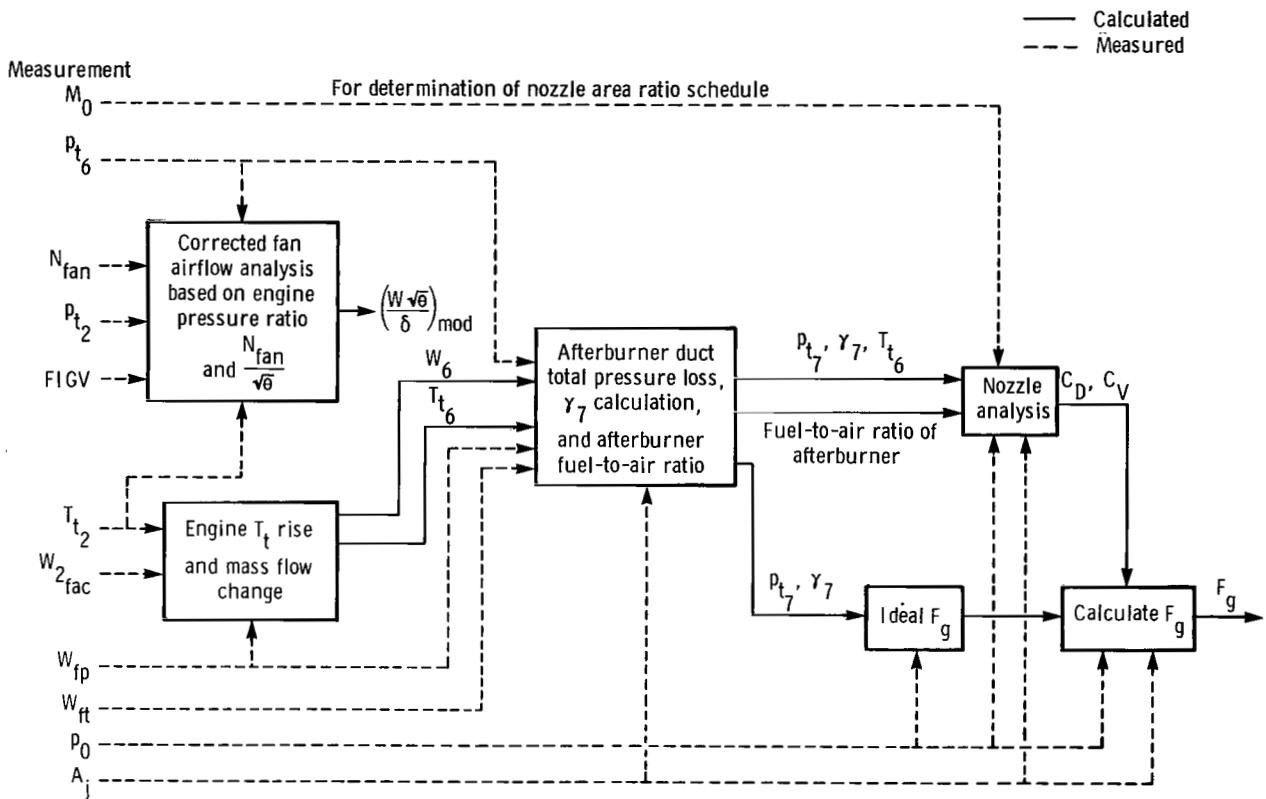


Figure 5. Engine performance calculation model.

function of engine core fuel-to-air ratio and inlet temperature. An analysis of the afterburner flow characteristics provides nozzle inlet total pressure, p_{t7} , and the ratio of specific heats, γ_7 . These two parameters are combined with free-stream ambient pressure to determine an ideal gross thrust. Nozzle discharge and velocity coefficients are determined from p_{t7} , A_j , nozzle area ratio, and γ_7 . The fuel-to-air ratio of the afterburner and T_{t6} are used to determine nozzle thermal expansion.

The ideal thrust is combined with the nozzle coefficients to compute the actual gross thrust. The model was operated using the facility's value of engine airflow instead of the value calculated for the determination of gross thrust. This prevented uncertainties in the model's airflow calculation from affecting the gross thrust calibration.

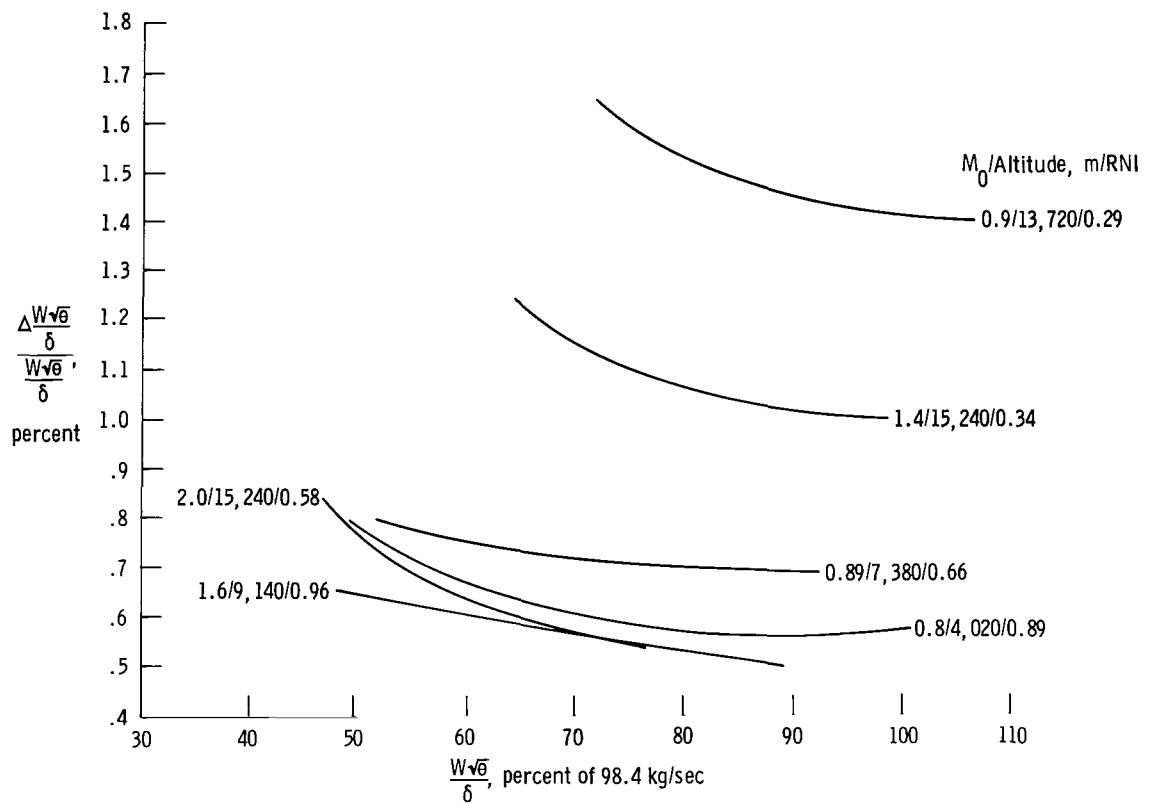
Reference 4 discusses the application of a gas generator method of this type on a similar engine and indicates the effect of measurement uncertainties on the thrust computation.

FACILITY AND MODEL UNCERTAINTY

Facility Uncertainty

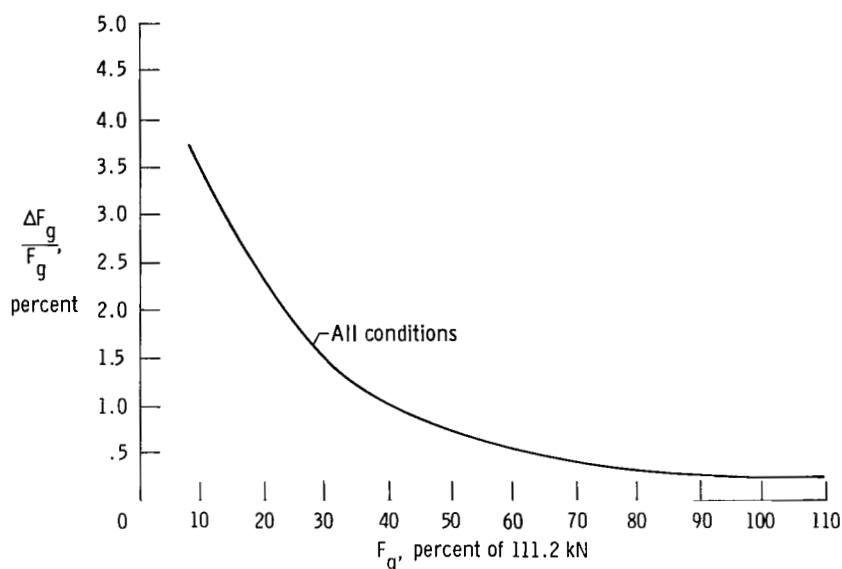
Figures 6(a) and 6(b) show the uncertainties of the facility-measured corrected engine airflow and gross thrust for several test conditions. The procedure for the determination of these values can be found in reference 1. Facility-corrected airflow uncertainty for the bulk of the data was less than 0.8 percent but increased to 1.7 percent for low Reynolds number index (RNI) points. In general, uncertainty increased with decreasing RNI.

Facility gross thrust uncertainty ranged from 3.7 percent to less than 0.5 percent. The values of uncertainty generated a single curve when they were plotted versus facility-measured gross thrust.



(a) Facility-measured corrected airflow.

Figure 6. Uncertainties of corrected airflow and gross thrust as measured in facility and calculated by model.



(b) Facility-measured gross thrust.

Figure 6. Continued.

Model Uncertainty

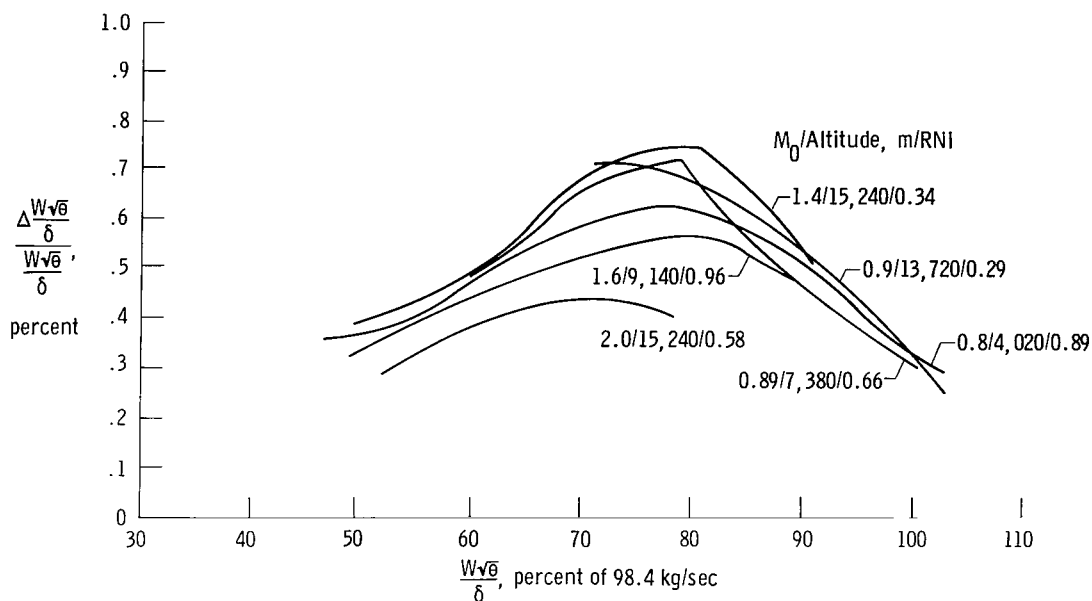
The uncertainties in the model-predicted values of corrected engine airflow and gross thrust were calculated for each data point. The model calculates uncertainty as the root sum square of the uncertainties due to each measurement uncertainty (table 2). (Corrected airflow uncertainty is normally not provided by the model, but the model was altered by NASA to provide this value.) Figures 6(c) and 6(d) show the characteristics of the model uncertainty for a cross section of engine test conditions. The uncertainty of the model-predicted corrected airflow was 0.7 percent or less. For each facility test condition, the uncertainty tended to peak in the region of 80 percent of design corrected airflow. Since the model used the facility-measured value of corrected engine airflow in its computation of gross thrust, a 1 percent overall uncertainty in facility-corrected engine airflow was assumed by the model for the computation of gross thrust uncertainty.

The model gross thrust uncertainty was as high as 5.2 percent, but generally fell below 3.8 percent. The values could be characterized by curves of constant RNI.

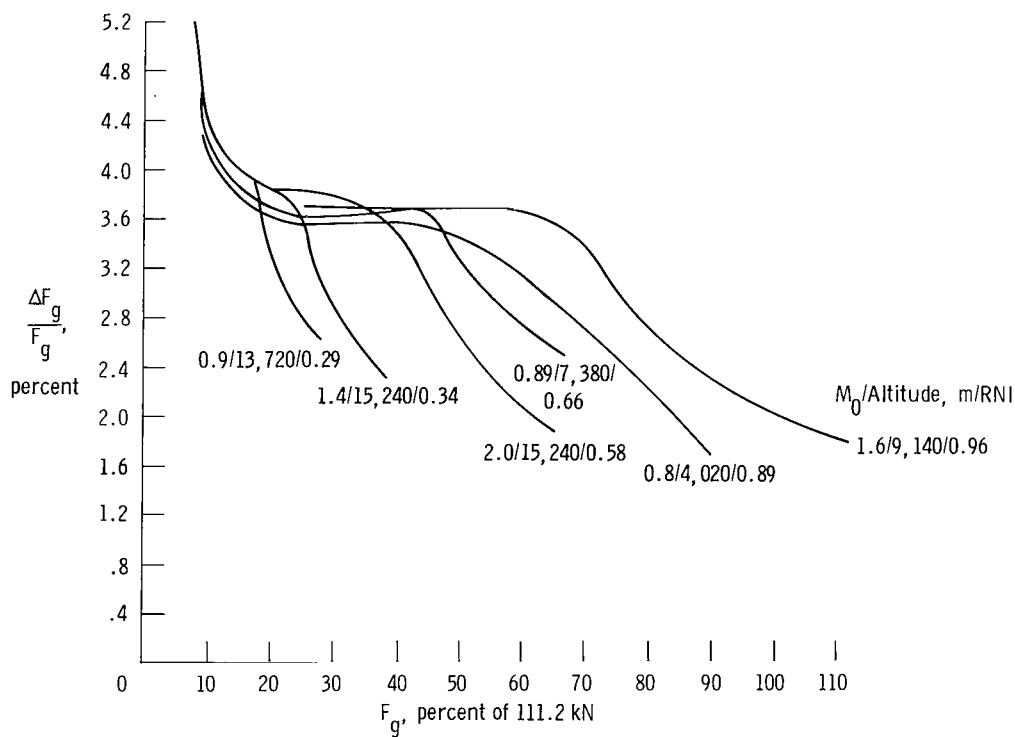
RESULTS AND DISCUSSION

Airflow Calibration

Figure 7 shows the corrected airflow calibration curves for engines 059 and 063 as functions of corrected fan speed. The engines exhibit the same general characteristics.

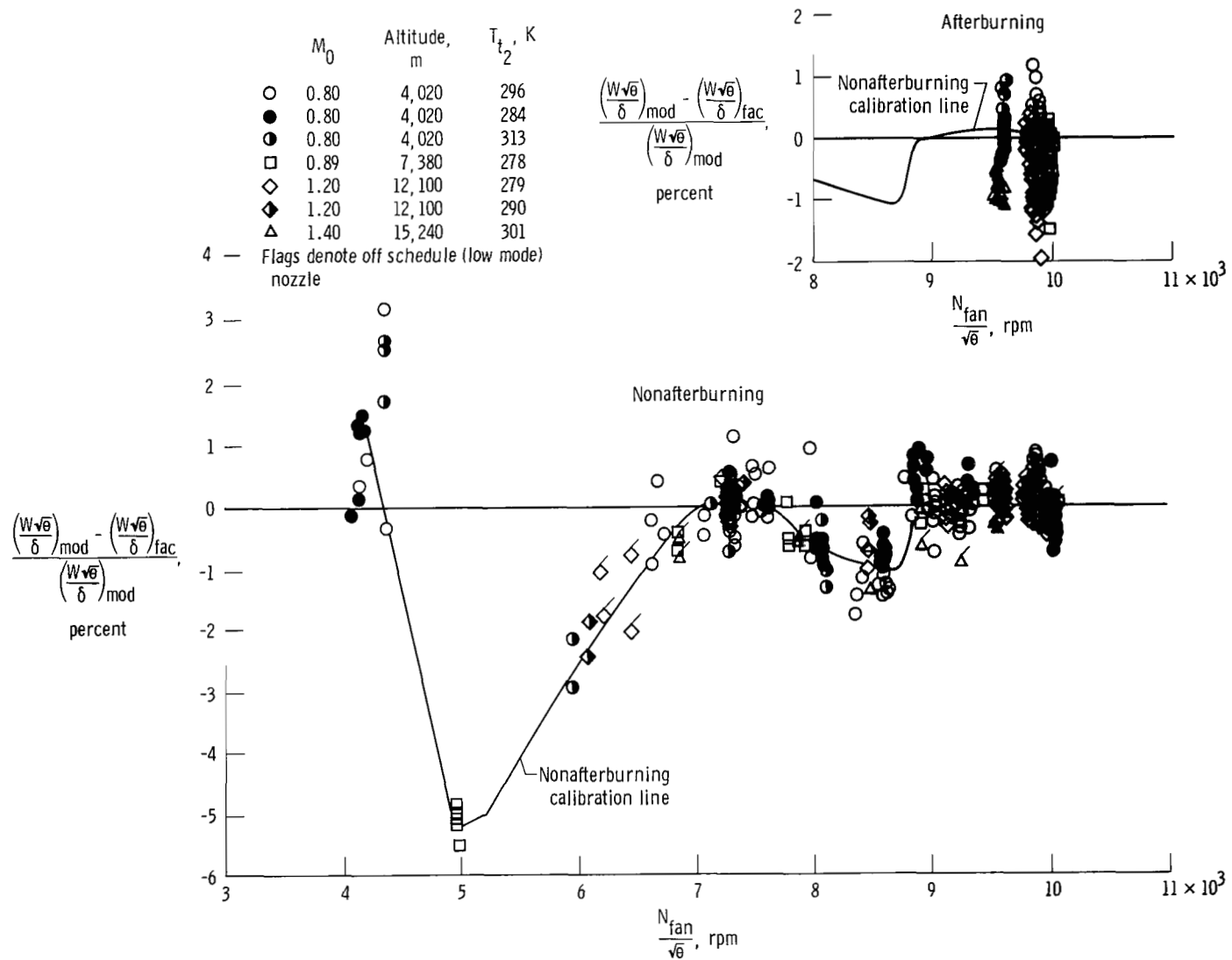


(c) Model-calculated corrected airflow.



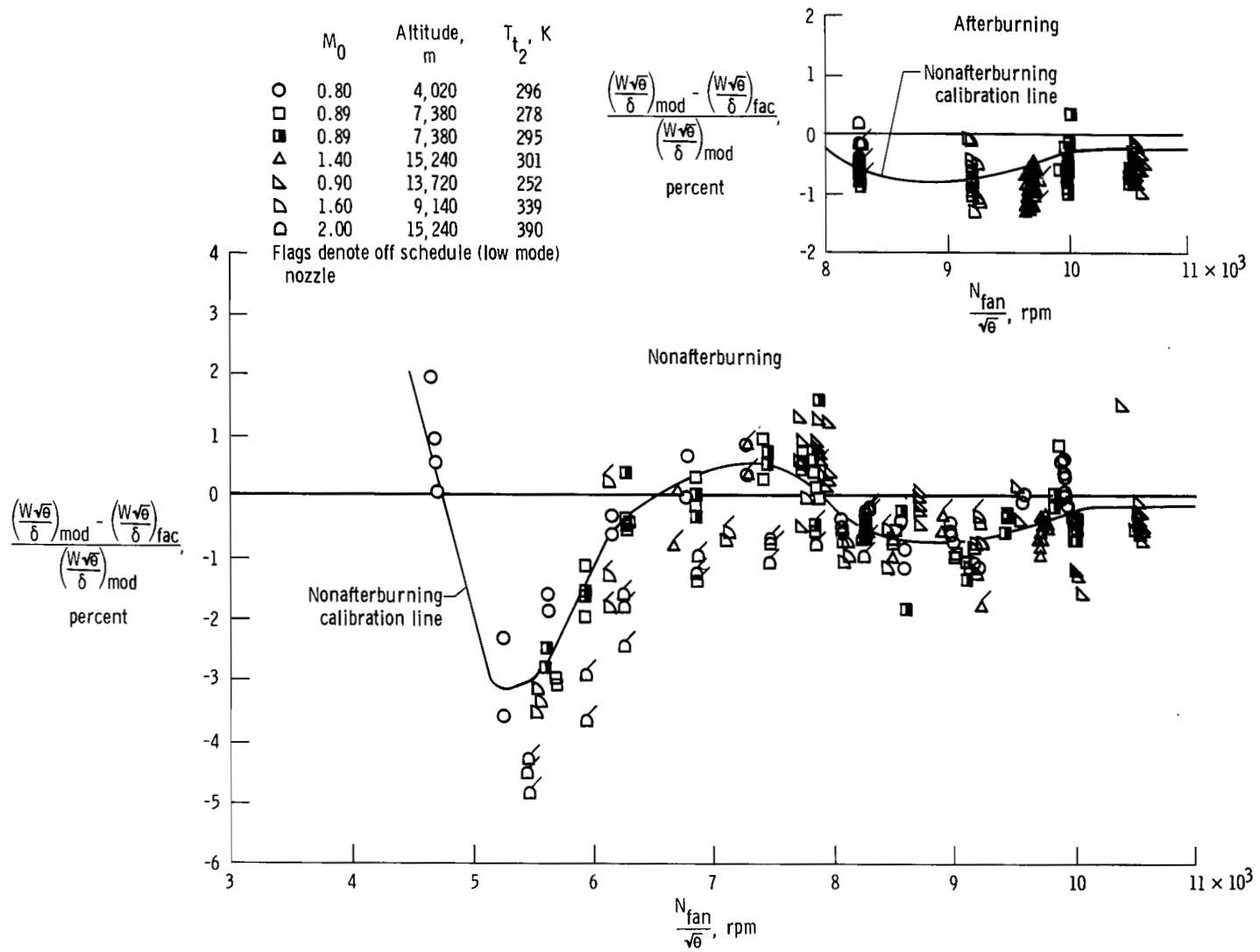
(d) Model-calculated gross thrust.

Figure 6. Concluded.



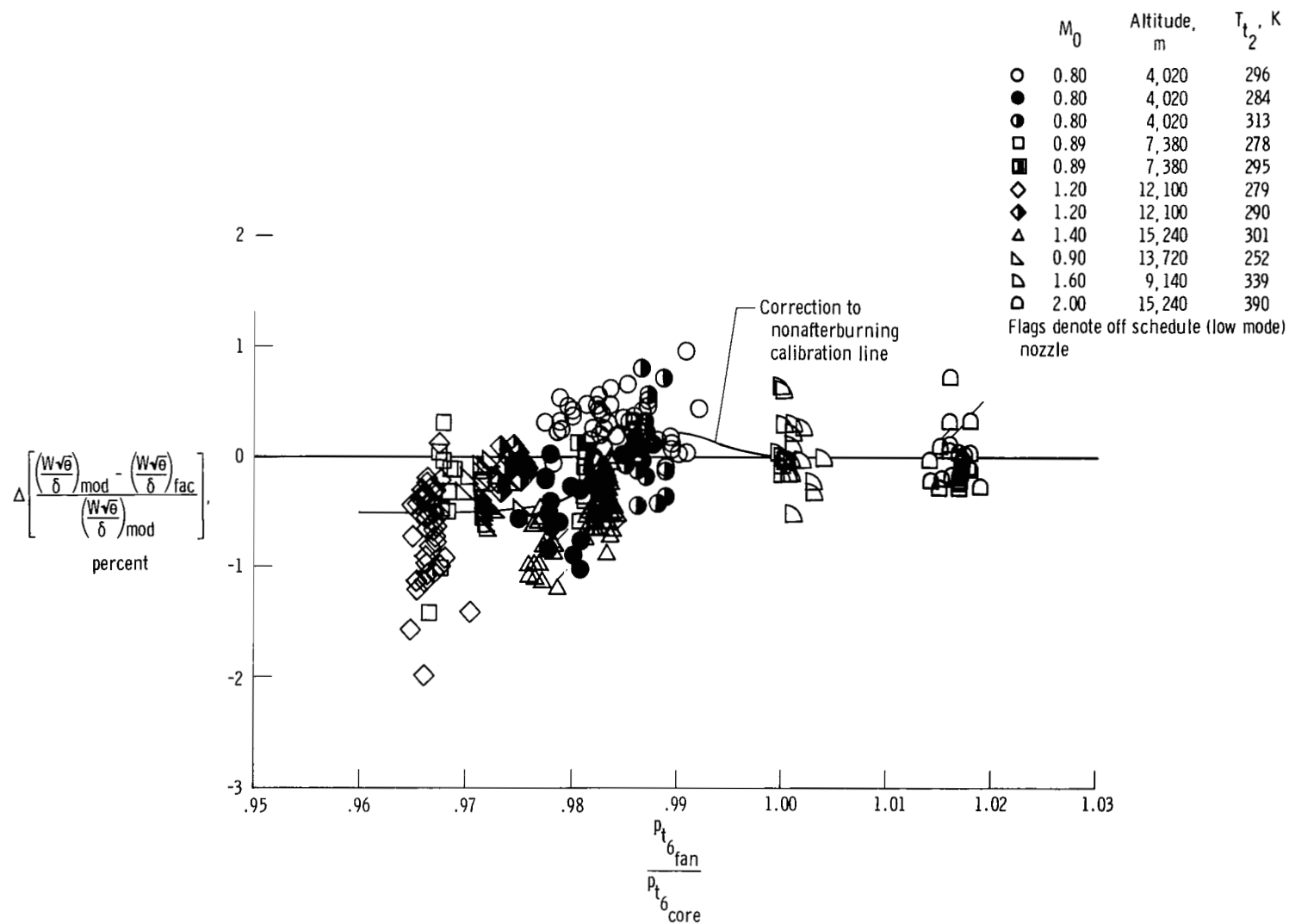
(a) Engine 059.

Figure 7. Corrected airflow calibration.



(b) Engine 063.

Figure 7. Continued.



(c) Engine 059 and 063. Correction to nonafterburning calibration line for afterburning.

Figure 7. Concluded.

The model calculation for the uncalibrated, average F100 engine predicts corrected engine airflow within ± 1 percent for most of the conditions tested on these two engines. For certain regions, however, there are significant discrepancies between the model-predicted and facility-measured values. Both engines indicate that the model underpredicts airflow by approximately 1 percent at corrected fan speeds near 8700 rpm, although the underprediction is more sharply pronounced for the conditions at which engine 059 was tested. The model underpredicts airflow by as much as 5 percent for engine 059 at a corrected fan speed of 5000 rpm, and by as much as 4.5 percent for engine 063 at a corrected fan speed of 5500 rpm. This characteristic is believed to be due to an error in the model airflow calculation for corrected fan speeds from 5000 rpm to 6000 rpm.

Figure 7(b) indicates that there is a shift in the calibration for engine operation at corrected fan speeds below 8000 rpm at the higher Mach numbers (Mach 2.00 at an altitude of 15,240 meters and Mach 1.60 at an altitude of 9140 meters). These values were not used to determine the calibration line, however, since nonafterburning operation at these conditions is of negligible importance in the flight program.

Corrected airflow characteristics during afterburning are also shown in figures 7(a) and 7(b). The calibration line is the calibration line for nonafterburning conditions. There is a measurable spread in the calibration data during afterburning operation, especially at the test conditions for engine 059. The correction to the nonafterburning calibration line from afterburning data is shown for both engines in figure 7(c). The correction to the nonafterburning calibration line was found to correlate with the ratio of average p_{t6} in the fan stream to average p_{t6} in

the core stream (fig. 3). This ratio is believed to reflect the assumption of uniform total pressure across both streams during afterburning operation. This characteristic may not characterize the average engine; it may be specific to these engines at these test conditions. Inlet total temperature variation of up to 17 K from standard day was observed to have no effect on the corrected engine airflow calibration.

Reynolds number.—Figure 8 compares the model-predicted and facility-measured effects of Reynolds number on airflow. The figure was obtained by taking

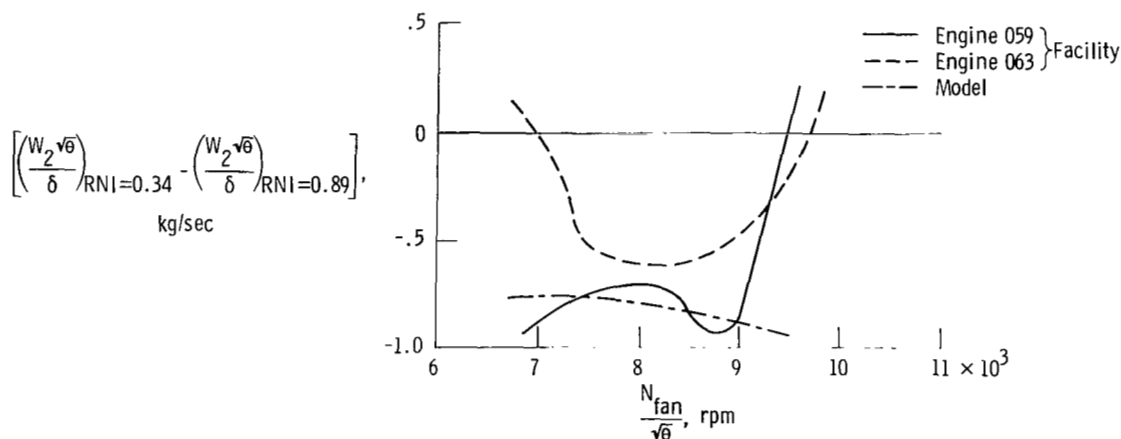


Figure 8. Reynolds number effect on corrected airflow.

the differences in the facility-measured and model-predicted airflow for Reynolds numbers of 0.89 (Mach 0.80, altitude 4020 meters) and 0.34 (Mach 1.40, altitude 15,240 meters). While basic data inaccuracy prevents the resulting differences in corrected airflow from being accurate, regions of the curve agree between model and facility. The differences in the detail of the curves may be due to curve fitting accuracy, engine schedule differences, or both.

As shown, operation at an RNI of 0.34 results in a loss of 0.6 to 0.9 kilogram per second in corrected airflow relative to an RNI of 0.89, as measured by the facility and predicted by the model.

Distortion effects.—Table 4 shows the effect of the 13.5 percent distortion screen on engine 059 at Mach 0.80 and an altitude of 4020 meters at intermediate power. The effect was determined by comparing the errors in the model prediction of corrected airflow, which does not include a correction for distortion. At intermediate power, the engine model overpredicts corrected engine airflow by about 1 percent over the undistorted values, indicating a 1 percent airflow loss.

TABLE 4.—CHANGE IN AIRFLOW WITH DISTORTION
AT INTERMEDIATE POWER

Engine	$\Delta \frac{W\sqrt{\theta}}{\delta}$, percent	D, percent
059	-1	13.5
063	0	26.5

Table 4 also shows the effect of the 26.5 percent distortion screen on engine 063 at Mach 0.89 and 7300 meters. No difference in airflow was observed between distorted and undistorted conditions.

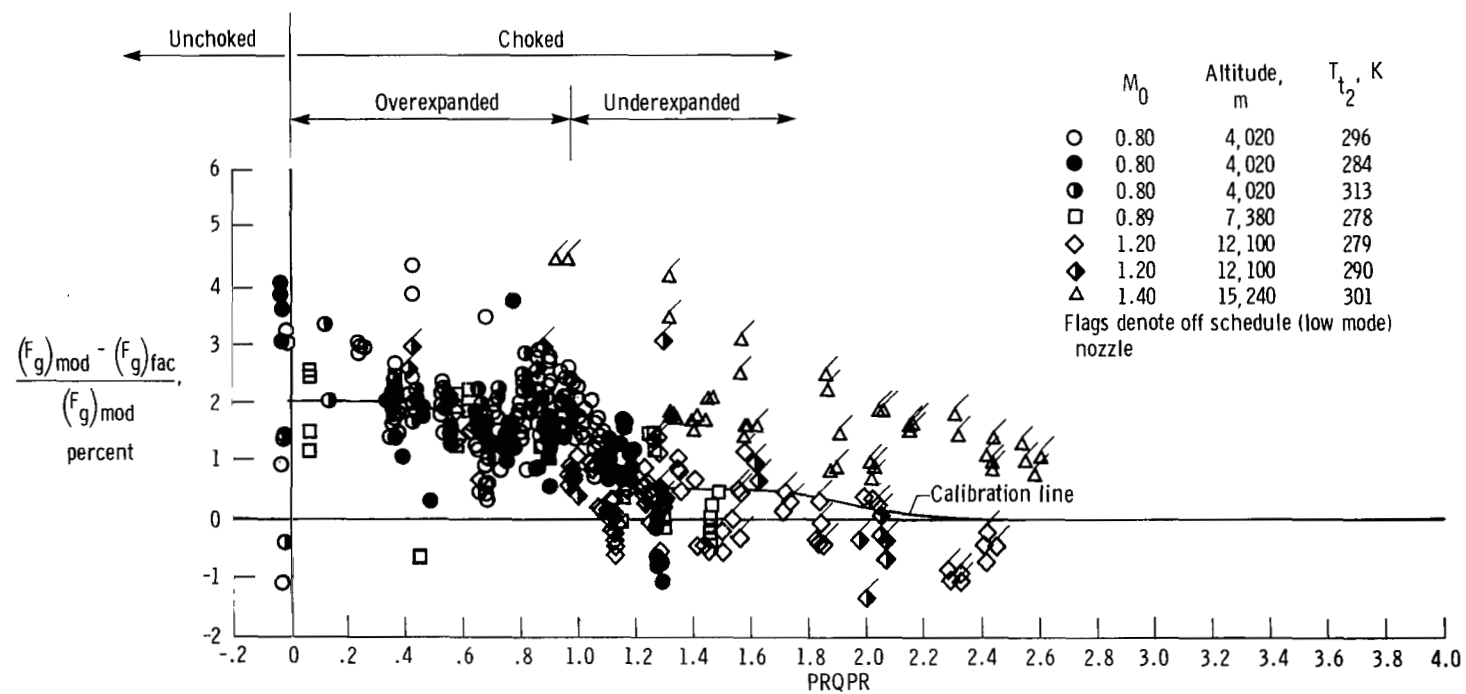
The differences between the engine 059 and 063 results are believed to be due to the effects of distortion pattern on the airflow at the fan, which are not taken into account by the distortion percentage value. The inability to correlate airflow changes with distortion in addition to a lack of sufficient data prevents the determination of a correction to airflow for distortion. It is felt that the changes in airflow with distortion will be less than or equal to 1 percent for F-15 flight test conditions.

Gross Thrust Calibration

Figure 9 shows calibrations for the model-predicted values of gross thrust for engines 059 and 063. The calibration coefficient is correlated with a parameter from the engine model called *PRQPR*, which is defined as follows:

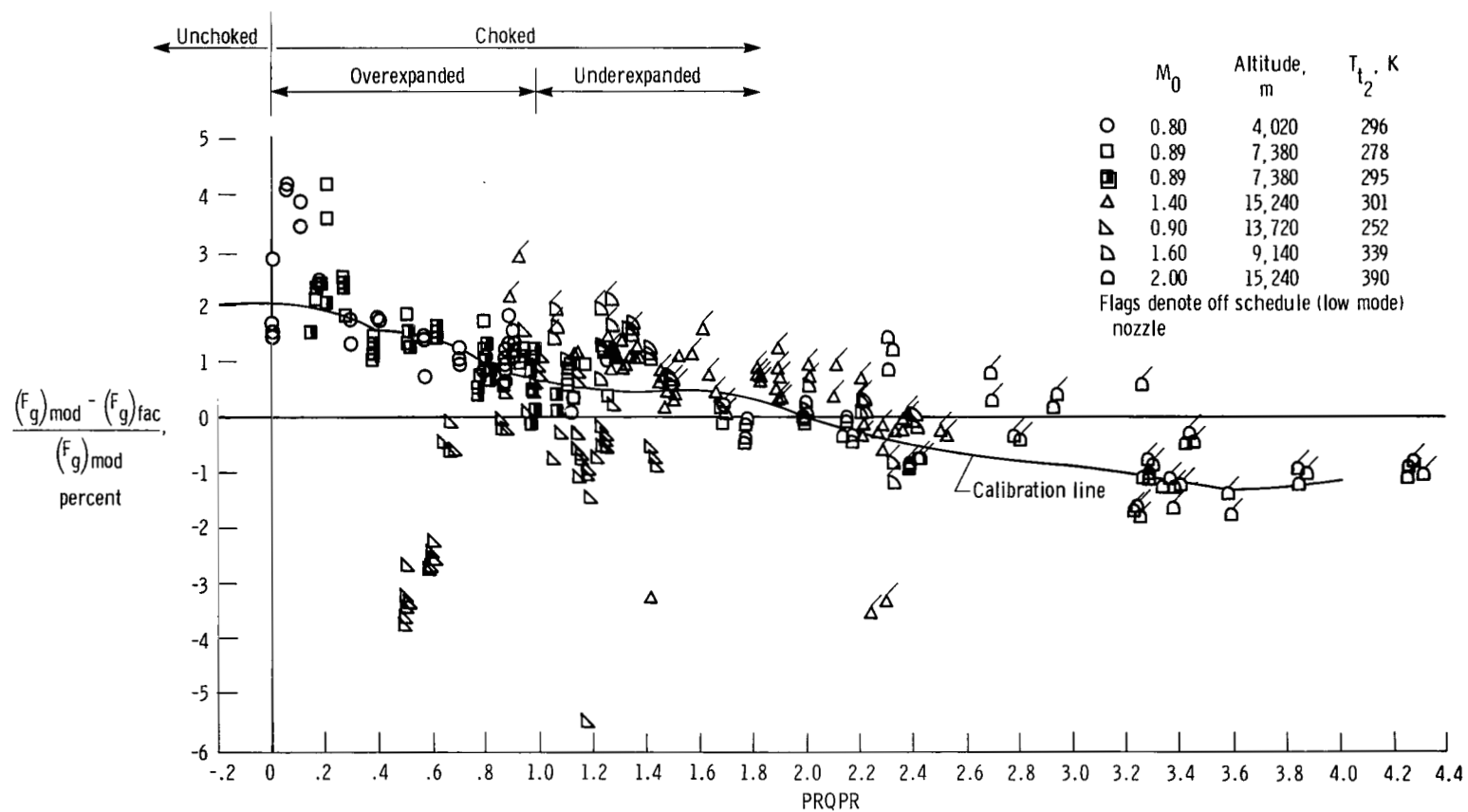
$$PRQPR = \frac{NPR - PR_{g_{sb}}}{PR_{g_{sp}} - PR_{g_{sb}}}$$

where NPR is the nozzle pressure ratio, $PR_{g_{sb}}$ is the nozzle exit pressure ratio if the flow is subsonically expanded (isentropically) through the effective nozzle



(a) Engine 059.

Figure 9. Gross thrust calibration.



(b) Engine 063.

Figure 9. Concluded.

ratio, $\frac{A_e}{A_j C_D}$, and $PR_{8_{sp}}$ is the nozzle exit pressure ratio if the flow is supersonically expanded (isentropically) through the effective nozzle area ratio. The station 8 pressure ratios are determined from $M_{8_{sb}}$ and $M_{8_{sp}}$, respectively, which reflect two possible solutions for expansion through the given effective area ratio. For the ideal case, $PRQPR < 0$ for unchoked nozzle operation, $PRQPR = 0$ for critical operation, $PRQPR = 0$ to 1 for an overexpanded choked nozzle, $PRQPR = 1$ for a properly expanded choked nozzle, and $PRQPR > 1$ for an underexpanded choked nozzle. The $PRQPR$ parameter generally provided a consistent collapse of data throughout the range of engine operating conditions.

Both engines show the same general trends, depending on the type of nozzle operation. When the nozzle was overexpanded, the model overpredicted thrust by 1 percent to 3 percent. The accuracy of the model was generally ± 2 percent once the nozzle became underexpanded.

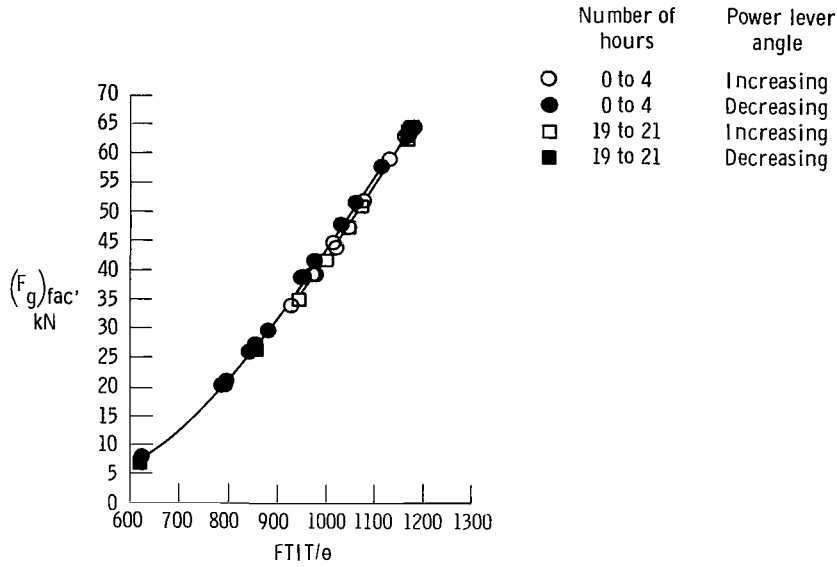
At Mach 1.40 at an altitude of 15,240 meters, the standard day nonafterburning data taken on engine 059 required a positive 2 percent shift in the model calibration. This deviation was not as pronounced for engine 063 at the same test conditions. The trend is unexplained. The data were not included in the determination of the calibration line.

The data for the Mach 0.90, 13,720-meter standard day for engine 063 (fig. 9(b)) indicate that the model significantly underpredicts thrust (by up to 3.5 percent) at values of $PRQPR$ between 0.4 and 0.7. However, the uncertainty of the facility measurements is high at this test condition because of the low value of engine gross thrust (fig. 6(b)). These data were also excluded when the calibration line was determined.

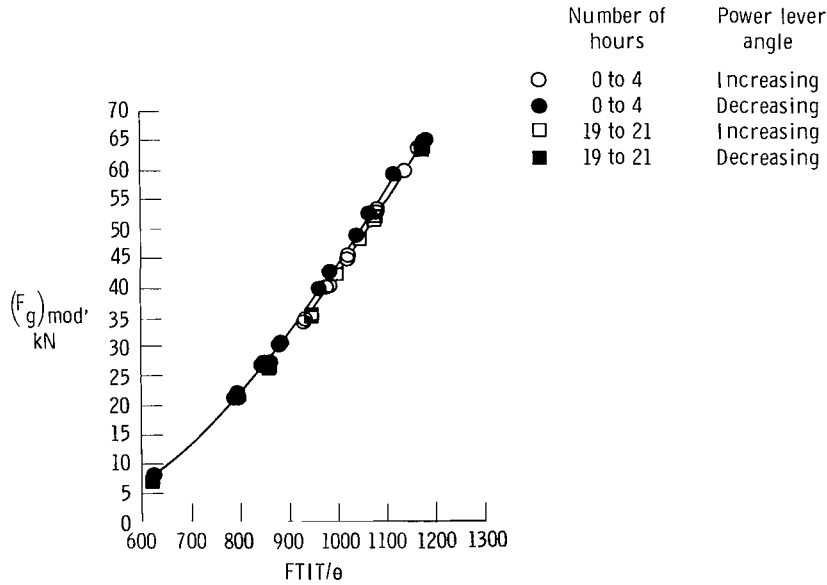
Engine Hysteresis and Degradation

Figure 10 indicates the hysteresis and degradation characteristics for engine 059 plotted against $FTIT/\theta$. The hysteresis data were acquired in sequentially decreasing and increasing steps of power lever angle at Mach 0.80, 4020-meter, standard day, undistorted inlet conditions. The data indicate hysteresis of approximately 0.9 kilonewton. The indicated hysteresis is the same for both facility-measured and model-calculated gross thrust, indicating that the hysteresis is a characteristic of engine 059 and not the facility. Since the model and the facility agree, the hysteresis had no noticeable effect on the gross thrust calibration.

An attempt to observe engine degradation was made by comparing data for the same operating conditions after 20 hours of engine operation. Data were acquired only with sequentially increasing steps of power lever angle. No degradation was observed.



(a) Based on facility-measured F_g .



(b) Based on model-calculated F_g .

Figure 10. Hysteresis and degradation for engine 059.
 $M_0 = 0.80$, altitude = 4020 m, $T_{t_2} = 296$ K.

Statistical Validation of Results

Table 5 provides values of 2σ , or twice standard deviation, and average deviation for the airflow and thrust model's calculation with and without the calibration.

TABLE 5.—PERFORMANCE MODEL CALCULATION ACCURACY

(a) Engine 059

Parameter	Model	2σ	Average deviation
$\frac{w\sqrt{\theta}}{\delta}$	Calibrated	1.24	0.43
	Uncalibrated	1.72	0.54
F_g	Calibrated	1.94	0.64
	Uncalibrated	3.51	1.50

(b) Engine 063

Parameter	Model	2σ	Average deviation
$\frac{w\sqrt{\theta}}{\delta}$	Calibrated	1.17	0.40
	Uncalibrated	2.16	0.81
F_g	Calibrated	2.38	0.71
	Uncalibrated	2.73	1.06

The calibrated model's calculation of corrected airflow has a 2σ value of 1.24 percent for engine 059 and 1.17 percent for engine 063. The 2σ value for gross thrust is 1.94 percent for engine 059 and 2.38 percent for engine 063. The uncalibrated model calculation of airflow has a 2σ value of 1.72 percent for engine 059 and 2.16 percent for engine 063. The 2σ value for gross thrust is 3.51 percent for engine 059 and 2.73 percent for engine 063. These values were calculated using all the data shown except for the distorted inlet conditions.

It was desirable to compare the accuracy of the model's calculations with uncertainties estimated for the facility and model due to instrumentation. To accomplish this, the uncertainty due to instrumentation was calculated for each data point. All these uncertainty values were then root sum squared. The final values for the facility, model, and facility and model combined are shown in table 6 for engine 063. When these values are compared with the 2σ values described above, the values for corrected airflow agree within 0.14 percent, whereas the values for gross thrust differ by about 1.6 percent.

TABLE 6.—ENGINE 063 PERFORMANCE UNCERTAINTY
ESTIMATED FROM INSTRUMENTATION UNCERTAINTIES

Parameter	Facility	Model	Combined
	Root-sum-squared uncertainty		
$\frac{w\sqrt{\theta}}{\delta}$	0.93	0.46	1.03
F_g	1.91	3.44	3.94

One of the most significant factors affecting the model-predicted values of gross thrust is nozzle area, A_j . A comparison of two independent A_j measurements on engine 063 indicated a repeatability (randomness) of 1 percent. The uncertainty of A_j in table 2, however, is large enough to represent the possible uncertainty in the A_j measurement on the average engine, which includes bias errors. The accuracy of the calibration on one engine is determined by the repeatability of the instrumentation in that engine, since the bias error is absorbed in the calibration. This is believed to be the major reason for the difference between the estimated uncertainty and the actual accuracy.

Although this method of root sum squaring the uncertainties at each data point is based on several assumptions about the nature of the various uncertainties, the most important being that the errors are independent, it provides a fairly realistic value for performance uncertainty for this type of test.

CONCLUDING REMARKS

Airflow and gross thrust calibrations were determined for two F100-PW-100 prototype engines in an altitude test facility. The data were used to provide a calibration for an engine model; the calibrated engine model had twice standard deviation (2σ) accuracies of approximately 1.24 percent for corrected airflow and 2.38 percent for gross thrust.

The uncalibrated engine model underpredicted airflow for low corrected fan speeds, and overpredicted gross thrust by an average of 2 percent for overexpanded nozzle operation. Overall, the uncalibrated average engine model had 2σ values of approximately 2 percent for corrected airflow and 3.5 percent for gross thrust.

Distortion effects were small and uncorrelatable. The Reynolds number index variation from 0.89 to 0.34 resulted in a reduction of corrected airflow of less than 1 kilogram per second, as was predicted by the engine model. Hysteresis was observed, but had no apparent effect on the calibration. Engine degradation was not measurable. The accuracy of the calibration was consistent with the uncertainty estimated from instrumentation measurement uncertainty.

*Dryden Flight Research Center
National Aeronautics and Space Administration
Edwards, Calif., June 2, 1978*

REFERENCES

1. Biesiadny, Thomas J.; Lee, Douglas; and Rodriguez, Jose R.: Airflow and Thrust Calibration of an F100 Engine, S/N P680059, at Selected Flight Conditions. NASA TP-1069, 1978.
2. Biesiadny, Thomas J.; Lee, Douglas; and Rodriguez, Jose R.: Altitude Calibration of an F100, S/N P680063, Turbofan Engine. NASA TP-1228, 1978.
3. F100 (3) In-Flight Thrust Calculation Deck. CCD 1088-2.0, Pratt & Whitney Aircraft, 1975.
4. Burcham, Frank W., Jr.: An Investigation of Two Variations of the Gas Generator Method To Calculate the Thrust of the Afterburning Turbofan Engines Installed in an F-111A Airplane. NASA TN D-6297, 1971.

1. Report No. NASA TP-1373		2. Government Accession No.		3. Recipient's Catalog No.	
4. Title and Subtitle COMPARISON OF CALCULATED AND ALTITUDE-FACILITY-MEASURED THRUST AND AIRFLOW OF TWO PROTOTYPE F100 TURBOFAN ENGINES				5. Report Date December 1978	
				6. Performing Organization Code	
7. Author(s) Frank J. Kurtenbach				8. Performing Organization Report No. H-1015	
9. Performing Organization Name and Address NASA Dryden Flight Research Center P.O. Box 273 Edwards, California 93523				10. Work Unit No. 505-11-24	
				11. Contract or Grant No.	
				13. Type of Report and Period Covered Technical Paper	
12. Sponsoring Agency Name and Address National Aeronautics and Space Administration Washington, D.C. 20546				14. Sponsoring Agency Code	
15. Supplementary Notes					
16. Abstract <p>Two F100-PW-100 prototype afterburning turbofan engines were airflow and thrust calibrated in the NASA Lewis Research Center Propulsion Systems Laboratory 4 altitude facility. The engines were calibrated to support flight research at the Dryden Flight Research Center.</p> <p>This report compares the facility performance data for the two engines with an engine performance model, and it provides corrections that can be applied to the model so that it represents the test engines accurately over the flight envelope. Test conditions ranged from Mach numbers of 0.80 to 2.00 and altitudes from 4020 meters to 15,240 meters. Two distortion screens were used to determine the effect of distortion on airflow. Reynolds number effects were also determined. Engine hysteresis is documented, as is an attempt to determine engine degradation.</p> <p>The calibrated engine model had a twice standard deviation accuracy of approximately 1.24 percent for corrected airflow and 2.38 percent for gross thrust.</p>					
17. Key Words (Suggested by Author(s)) Thrust Engine performance Airflow				18. Distribution Statement Unclassified—Unlimited	
STAR Category: 07					
19. Security Classif. (of this report) Unclassified		20. Security Classif. (of this page) Unclassified		22. Price* \$3.75	
				21. No. of Pages 30	

*For sale by the National Technical Information Service, Springfield, Virginia 22161

NASA-Langley, 1978

National Aeronautics and
Space Administration

THIRD-CLASS BULK RATE

Postage and Fees Paid
National Aeronautics and
Space Administration
NASA-451



Washington, D.C.
20546

Official Business

Penalty for Private Use, \$300

8 1 10, A, 112078 S00903DS
DEPT OF THE AIR FORCE
AF WEAPONS LABORATORY
ATTN: TECHNICAL LIBRARY (SUL)
KIRTLAND AFB NM 87117

NASA

POSTMASTER: If Undeliverable (Section 158
Postal Manual) Do Not Return

S